Plant Reproduction
https://doi.org/10.1007/s00497-021-00404-5

METHODS PAPER

A simple and rapid method for imaging male meiotic cells in anthers of model and non-model plant species

Claudia Rossig[1] · Liam Le Lievre[1] · Sarah M. Pilkington[2] · Lynette Brownfield[1]

Received: 21 October 2020 / Accepted: 27 January 2021

Key message **We describe a simple method to view meiotic cells in whole anthers from a range of plants. The method retains spatial organisation and enables simultaneous analysis of many meiotic cells.**

Abstract Understanding the process of male meiosis in flowering plants, and the role of genes involved in this process, offers potential for plant breeding, such as through increasing the level of genetic variation or the manipulation of ploidy levels in the gametes. A key to the characterisation of meiotic gene function and meiosis in non-model crop plants, is the analysis of cells undergoing meiosis, a task made difficult by the inaccessible nature of these cells. Here, we describe a simple and rapid method to analyse plant male meiosis in intact anthers in a range of plant species. This method allows analysis of numerous cells undergoing meiosis and, as meiotic cells stay within the anther, it retains information of the three-dimensional organisation and the location of organelles in meiotic cells. We show that the technique provides information on male meiosis by looking at the synchrony of meiotic progression between and within locules, and comparing wildtype and mutant plants through the chromosome separation stages in *Arabidopsis thaliana*. Additionally, we demonstrate that the protocol can be adopted to other plants with different floral morphology using *Medicago truncatula* as an example with small floral buds and the non-model plant kiwifruit (*Actinidia chinensis*) with larger buds and anthers.

Keywords Male meiosis · Meiocytes · Anther · Confocal laser scanning microscopy · Fluorescent staining

Introduction

Meiosis is essential in sexual reproduction in eukaryotes (Harrison et al. 2010). It reduces the chromosome content in gametes and increases genetic variation. Meiosis involves a single round of DNA replication, an extended prophase where pairing and recombination between homologous chromosomes exchanges genetic information, followed by two rounds of chromosome separation. The first separation, meiosis I, is reductional and involves the separation of homologous chromosomes, while the second division, meiosis II, is equational being similar to mitosis as it involves the separation of sister chromatids.

Male meiosis in plants occurs within the anther compartment of the flower. Each anther is a bilaterally symmetrical structure with four lobes or locules with distinct cell layers: epidermis (outermost), endothecium, middle layer, tapetum and sporogenous cells (innermost) (Goldberg et al. 1993; Wilson et al. 2011). The sporogenous cells develop into pollen mother cells which become separated from the tapetum and undergo meiosis. In *Arabidopsis thaliana,* meiosis takes around 24 h, with the prophase stages taking the majority of the time (Armstrong et al. 2003). Cytokinesis in plant male meiosis can be either successive, occurring after each round of chromosome separation, or simultaneous, with one round of cytokinesis after both chromosome separations (De Storme and Geelen 2013). Successive cytokinesis is common among monocots while simultaneous cytokinesis often occurs in eudicots. In meiocytes undergoing simultaneous cytokinesis, a band of organelles is formed between the two chromosome sets at the end of meiosis I which acts as a physical barrier to ensure proper chromosome separation throughout meiosis II (Brownfield et al. 2015). Following cytokinesis, each meiotic product develops into a pollen grain (Smyth et al. 1990).

Communicated by Raphael Mercier.

✉ Lynette Brownfield
lynette.brownfield@otago.ac.nz

[1] Department of Biochemistry, University of Otago, Dunedin, New Zealand

[2] The New Zealand Institute for Plant & Food Research Ltd (PFR), Private Bag 92169, Auckland 1142, New Zealand

Published online: 18 February 2021

Meiosis is highly dynamic and requires coordinated execution of conserved processes. Defects can have dramatic consequences such as unbalanced chromosome segregation producing aneuploid cells, impaired male fertility and unreduced gametes (Lei and Liu 2020). Thus, characterisation of genes involved in meiosis has been a goal in plant reproductive research and understanding the genetic variation in plants (Harrison et al. 2010; Crismani et al. 2013; Lambing and Heckmann 2018; Prusicki et al. 2019). Additionally, greater knowledge of the mechanisms underlying male meiosis in plants offers potential to manipulate the genetics of pollen used in plant breeding, for example increasing recombination rates or producing unreduced gametes to enable interploidy crosses or alter ploidy levels (Crismani et al. 2013; Lambing and Heckmann 2018). To date, much of the research into plant meiosis has occurred in the model eudicot *A. thaliana* as well as the monocot crop plants rice (*Oryza sativa*) and maize (*Zea mays*) (Lambing and Heckmann 2018). For maximum benefit, this research needs to be translated into a broad range of crop plants.

Genetic and genomic approaches have been, and will continue to be, crucial in uncovering key genes and processes in meiosis (Harrison et al. 2010; Crismani et al. 2013; Lambing and Heckmann 2018; Prusicki et al. 2019). Imaging of meiotic cells to observe the impact of mutations in genes and the impacts of environmental treatments on meiosis has been key in underscoring these genetic approaches (Lambing and Heckmann 2018). For our investigations into meiosis in *A. thaliana*, we wanted a relatively quick method to view numerous male meiocytes at the critical chromosome division stages (from the end of prophase I to cytokinesis). Further, to gain the most useful information this needed to be in a manner that maintained the three-dimensional structure of the meiotic cells, including the organelle band (Brownfield et al. 2015; Cabout et al. 2017).

Here, we describe the protocol we developed to do this using standard confocal laser scanning microscopy (CLSM) and intact anthers. We show the application of the protocol in the model species *A. thaliana*, focussing on the chromosome separation stages and observing the level of synchrony between anther locules and observing phenotypic effects of two mutations that impact spindle and organelle position during meiosis, *parallel spindle 1* (*ps1*) and *jason* (*jas*) (d'Erfurth et al. 2008; De Storme and Geelen 2011; Brownfield et al. 2015). Further, as translating meiotic knowledge into a range of plants with different floral morphology will be crucial to using meiosis to enhance plant breeding, we also show that the protocol can be adopted to other eudicots by imaging meiocytes in the model legume *Medicago truncatula* and the non-model crop plant kiwifruit (*Actinidia chinensis*).

Materials and methods

Plant material and growth

A. thaliana Columbia-0 (Col-0) and Landsberg *erecta* (L*er*) plants and *M. truncatula* ecotype Jemalong A17 plants were grown in soil at 20 to 22 °C under a 16-h-light and 8-h-dark cycle with approximately 70% relative humidity. *M. truncatula* plants were vernalised to facilitate flowering by placing scarified seeds on moist filter paper in a petri dish, incubated for 2 weeks at 4 °C before being transferred to soil (Barker et al. 2006). The *A. thaliana* mutants were in the Col-0 background and were the *ps1-1* allele (SALK_078818) and the *jas-3* allele (SAIL_813_H03) as previously described (d'Erfurth et al. 2008; Erilova et al. 2009).

Kiwifruit (*Actinidia chinensis* cv. Bruce) buds were taken from budwood grown in indoor growth rooms. Kiwifruit canes were collected from mature (at least 6-year-old) kiwifruit vines from the Plant & Food Research orchard in Motueka, New Zealand, (41° 9′ S, 172° 98′ E). Canes were stored in the dark at 4 °C for at least 1 month. For floral induction, canes with at least 10 mm basal diameter were cut into sticks of approximately 15 cm in length. Proximal ends of sticks were placed in 100 ml autoclaved distilled water and aerated at 20 °C with a 16-h-light and 8-h-dark cycle.

Collection and fixation of buds/anthers

Healthy *A. thaliana* inflorescences were removed using fine forceps from plants that had not entered senescence. Open flowers were removed before the inflorescences were placed into a 1.5 ml microcentrifuge tube (5–10 inflorescences per tube) with ~ 1 ml of Carnoy's solution (3:1 ethanol: acetic acid).

For *M. truncatula*, fine forceps were used to remove flower buds of approximately 1-mm length, as these are likely to contain meiotic anthers, and the buds immersed in Carnoy's solution in a 1.5 ml microcentrifuge tube (10–20 buds per tube).

For kiwifruit, buds in the size range of 3.5 mm to 4.5 mm in transverse diameter with compact green sepals were used as these most likely contain anthers with meiotic cells (Caporali et al. 2019). Buds were removed from the cane, opened and 20–30 anthers removed and placed in Carnoy's solution in a 1.5 ml microcentrifuge tube. Alternatively, a scalpel was used to cut a small 'window' into the side of a flower bud (through the tepals and sepals) still attached to the cane. Up to five anthers were removed through the window using fine forceps and transferred into Carnoy's solution.

The *A. thaliana* inflorescences, *M. truncatula* flower buds or kiwifruit anthers were incubated in Carnoy's solution for approximately 3–4 h at room temperature. The fixative was then replaced with fresh solution every few hours until the removed fixative was clear. Fixed material was stored at 4 °C.

Preparation and staining of anthers with meiotic cells

For *A. thaliana*, three or four fixed inflorescences were carefully transferred with forceps to a hand-polished microscope slide in a few µl of ddH_2O. Working with fine needles under a dissecting microscope, all buds with any yellow anthers were removed as these contain microspores or developing pollen. The next three or four oldest/biggest buds (around flower stage 9; Sanders et al. 1999) were selected for dissection. These buds were opened by removing the sepals and the filament of each stamen was cut. All non-anther material was removed from the slide, especially big debris that would raise the coverslip. To stain *A. thaliana* anthers, excess water was carefully removed from the slide using a small syringe or pipette and 20 µl of DAPI staining solution (0.4ug/ml DAPI (2-(4-Amidinophenyl)-6-indolecarbamidine dihydrochloride, Sigma-Aldrich #D9542), in 100 mM sodium phosphate, pH7.0, 1 mM EDTA, 0.1% (v/v) Triton X-100) was added. After 5 min, a coverslip (22 × 22 mm, thickness 0.13–0.16 mm) was added from above (to avoid anthers moving with the meniscus and being lost), taking care not to press against the anthers (requires a sufficient amount of liquid). Excess staining solution was removed by blotting with a Kimwipe and the microscope slide sealed with nail varnish. Slides were viewed the same day they were prepared (we did not investigate whether they can be stored).

M. truncatula buds contain ten stamens arranged in a diadelphous fashion (nine stamens filaments are joined) around the pistil (Nair et al. 2008; Cardarelli and Cecchetti 2014). For analysis, five to ten fixed buds were transferred into a few µl of ddH_2O on a microscope slide and each flower bud opened with fine forceps. The upper, separated region of each filament was cut with fine forceps or a needle, and anthers with any yellow color were removed as these most likely contained post-meiotic stages. All non-anther material was removed from the slide and anthers were stained with DAPI in the same manner as *A. thaliana* anthers.

For kiwifruit anthers, the fixative was carefully aspirated without disrupting anthers. The anthers were then washed once with PBS pH 7.0, before being suspended in 50 µl of DAPI/Mowiol/Glycerol staining solution (DAPI solution as above with 5% (w/v) Mowiol 4–88 and 12% (v/v) Glycerol) and incubated for 15 min in the dark. No more than ten kiwifruit anthers were added to a single slide, to ensure the mass of the material did not cause the cover slip to raise above the mount and the glycerol assisted with the movement and positioning of anthers on the slides. A coverslip was quickly added to avoid the staining solution becoming too viscous and sealed with nail varnish. Slides were viewed on the same day.

All material was kept wet during processing to avoid the anthers drying out as this leads to high levels of autofluorescence.

Confocal microscopy of meiotic cells

The slides can be viewed on any standard CLSM set up with lasers and filters for the excitation (405 nm) and emission for DAPI (415–470 nm). We used an Olympus FluoView FV1000 microscope with Olympus FluoView software with pre-set settings for DAPI. Images were captured with UPLSAPO 20X, UPLSAPO 40X or PLAPON 60X O SC objective lenses.

Microscope slides were screened with low magnification (10 or 20×) with white light. For pre-meiotic anthers (based on size) and anthers with young microspores (based on the visible microspore walls or high opacity) were not further analysed. Anthers in which the meiotic stage could not be determined under white light, or with epifluorescence, due to the multiple cell layers surrounding meiotic cells, were chosen for further analysis.

For selected anthers, the magnification was increased, and the anthers viewed with CLSM. Preliminary screens were conducted with a brief dwell time (around 4 µsec/pixel), a high gain setting (2 to 4x) and the photon multiplier detector set to ~ 650 mV, to limit bleaching of the sample material. When an anther containing the target stage was identified, the region was selected, including the top and bottom for a z-series, and the focus adjusted. In our analysis, we wanted to be able to observe non-chromosomal DNA (i.e., in organelles), thus we determined the imaging conditions that enabled this: dwell time 12.5–20 µsec/pixel, the 1× gain and the photon multiplier detector set to ~ 500 mV, with the precise settings optimised for each anther. In addition, Kalman averaging (3–5 scans) was used to reduce background. These confocal settings resulted in some overexposure for some chromosomal DNA in meiocytes and some anther cells. We recommend researchers spend time optimising the CLSM settings for the features they wish to observe (chromosomal or organelle DNA).

To analyse images and look at meiotic features taking three-dimensional information into account, we used ImageJ to stack slices and make z-series. Adobe Photoshop was used to prepare figures.

Results and discussion

Whole anther analysis in *A. thaliana*

To analyse whole anthers containing meiotic cells from *A. thaliana*, we developed a simplified protocol that is summarised in Fig. 1, and described in detail in the Methods. Briefly, for *A. thaliana* this involved fixation of whole inflorescences, selection of buds with meiotic stage anthers (usually anthers of stages 5 and 6 or flower stage 9; Sanders et al. 1999), isolation of the anthers, staining of chromosomal and organelle DNA with DAPI, and imaging using standard CLSM techniques. Here, we report our findings with Col-0, with similar observations made with *A. thaliana* L*er* (Online Resources 1 and 2).

A. thaliana anthers contain four locules and meiotic cells undergo simultaneous cytokinesis. Using our protocol, parts of all four locules could be observed in a single optical section for some anthers (Fig. 2a, with the z-series for the same anther in Online Resource 3), while only two locules are visible in a single optical section from other anthers and a *z*-series was required to observe all four locules (Online Resource 4). Each locule contains many meiocytes at the same or similar stage, and this technique offers the opportunity to image a large number of cells at the same or similar stage, which is useful to compare

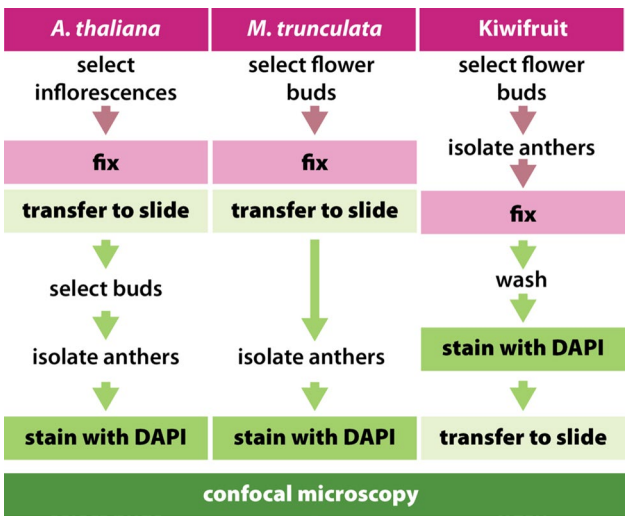

Fig. 1 Flow diagram showing the order of the main stages for the preparation and staining of whole anthers with meiotic cells with DAPI for CLSM for *A. thaliana*, *M. truncatula* and kiwifruit. The major steps of this method are similar for each plant, but the order of events differs due to different floral architecture. Both *A. thaliana* and *M. truncatula* have small floral buds and manipulation of isolated anthers difficult, so the anthers are not isolated from the bud and stained until after they are fixed and transferred to a microscope slide. Kiwifruit has bigger floral buds and bigger more robust anthers, so anthers are isolated prior to fixation and staining

mutants with wild-type plants. We focussed our analysis on the stages involving chromosome separation (the end of prophase I to anaphase II). With each microscope slide containing anthers from three to four inflorescences, we generally found several anthers on slides containing meiocytes in this target range.

Being able to observe all four locules in an anther allowed us to observe the level of developmental synchrony between the locules of an anther. Anthers with locules containing prophase stages (Online Resource 5) often appeared synchronised, consistent with these stages progressing over longer periods of time and reports of synchronous male meiosis in plants (Li et al. 2015; Armstrong et al. 2003; Bennett et al. 1971). However, in anthers containing the chromosome division stages, locules were often observed to contain meiocytes at different meiotic stages, even ranging from metaphase I to post-cytokinesis in a single anther (Fig. 2a, Online Resources 3). This likely reflects the short timeframe in which these meiotic divisions occur (Armstrong et al. 2003; Bennett et al. 1971), rather than significant developmental asynchrony between locules at these stages.

In some anthers, we also observed small differences of meiotic progression within a single locule with a gradient or wave of development (Fig. 2a, b, Online Resource 3). This was most commonly in locules in which the chromosome separation stages were in progress. For example, meiocytes being in the interphase between the two chromosome separations at one end of the anther and meiocytes at the other end with chromosomes aligned at metaphase II (Fig. 2a right locule, Fig. 2b). The direction of the gradients within a locule was not consistent; with the earlier meiotic stage being towards the filament in some locules (Fig. 2a) or the tip of the anther in others (Fig. 2b). As far as we know, such within locule gradients have not been reported before and we are not sure how, or if, developmental signals establish such gradients. However, it may provide an opportunity to study meiotic defects in the chromosome separation stages by being able to visualise the precise stage impacted and compare to nearby meiocytes within one locule.

In *A. thaliana*, the anther consists of four cell layers; an outer epidermis, endothelium, middle cell layer and tapetum (Wilson et al. 2011). While not the focus of our work, analysis of DAPI-stained anthers by CLSM could also be used to observe these cell layers (Fig. 2). In particular, the binucleate tapetal cells can be distinguished. The tapetal cell layer supports meiocyte development, and communication between the tapetum and meiotic cells is taking place. As, mutations that affect development of tapetal cells have resulted in defects in male meiosis (Lei and Liu 2020; Scott et al. 2004), it may be useful to visualise both the tapetum and meiotic cells simultaneously, using this method with CLSM setting optimised to distinguish features of different cell types.

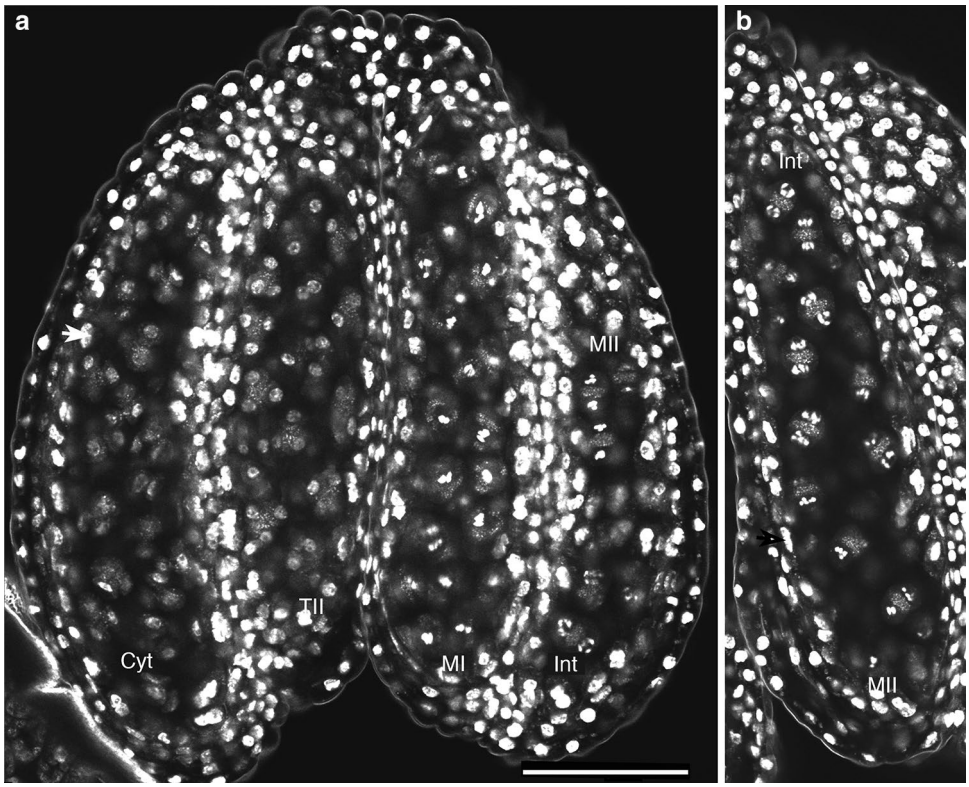

Fig. 2 CLSM analysis of meiocytes in *A. thaliana* anthers. Anthers were prepared from individual *A. thaliana* flower buds, chromosomal DNA and organelles stained with DAPI and observed with CLSM. **a** Whole anther showing different meiotic stages in each of the four locules. A *z*-series for this anther is provided in Online Resource 3 From left to right locules contain: meiotic products close to cytokinesis (Cyt); telophase II (TII) with the two meiotic divisions are complete (not all four nuclei are visible in the optical slice); metaphase I (MI) with homologous chromosomes aligned; Interphase (Int) between the two meiotic divisions at the bottom of the anther to metaphase II with two sets of sister chromatins aligned at the top (MII). Arrow indicates a binucleate tapetal cell. **b** A locule from another *A. thaliana* anther showing a gradient of meiosis stages from interphase (Int; top) to metaphase II (MII, bottom). Images are single optical sections. Scale; 50 µm

This method can also be used to focus on different meiotic stages and characterise the phenotypic impact of mutations with the *parallel spindle 1* (*ps1*; d'Erfurth et al. 2008) and *jason* (*jas*; De Storme and Geelen 2011, Brownfield et al. 2015, Cabout et al. 2017) used as examples here (Fig. 3; z-series for each image shown in Online Resources 5 to 22). In our analysis, we aimed to be able to observe both the chromosomal and organelle DNA, along with the overall organisation of meiotic cells. The amount of DNA in the organelles is less than in chromosomes and therefore organelles do not stain as brightly with DAPI. Our CLSM setting were optimised to be able to view the organelle DNA which has led to some overexposure of condensed chromosomal DNA. Altering the confocal setting (shorter dwell time, reduced detector sensitivity) could be used to prevent this overexposure for studies concentrating on the chromosomal DNA.

In the later stages of prophase (diakinesis), the wild type and two mutants were similar with bivalents observed and organelles distributed throughout the cytoplasm, although excluded from the nuclear regions (Fig. 3a–c, with bivalent in different planes shown in Online Resources 5–7). While our focus was on the chromosome separations stages, this indicates that some information on the prophase stages can be observed, particularly on the location of chromosomes within the cell and as a preliminary screen. However, if researchers are interested in detailed chromosome structure during prophase, and then we would recommend the use of well-established chromosomal spreading techniques (Fransz et al. 1998; Chelysheva et al. 2005; Colas et al. 2017).

At metaphase I, chromosomes can be observed aligned at the cell equator (Fig. 3d–f, Online Resources 8–10) with homologous chromosomes separating at anaphase I (Fig. 3g–i, Online Resources 11–13). The chromosome organisation is similar between wild type and the two mutants, although there appears to be more lagging chromosomes in the *ps1* mutant than in wild type or *jas*. While we have not quantified this, and lagging chromosomes are sometimes observed in wild-type meiocytes, it is consistent with the small nuclei observed in unbalanced meiotic

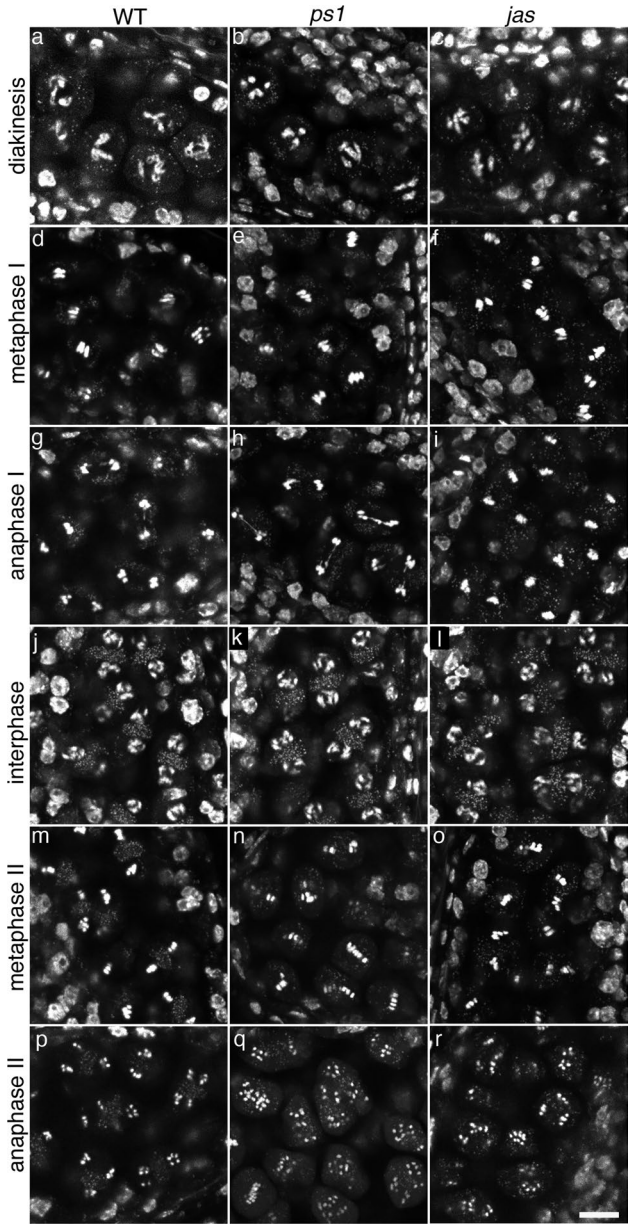

Fig. 3 *A. thaliana* meiocytes at different stages imaged within anthers. Chromosomal DNA structure and organelle DNA can be seen at diakinesis with bivalents visable (**a**–**c**); metaphase I with chromosomes aligned at the cell equator (**d**–**f**); anaphase I with homologous chromosomes separating (**g**–**i**); interphase with two groups of partially decondensed chromosomes with an organelle band between (**j**–**l**); metaphase II with two sets of chromosomes aligned on two spindles separated by an organelle band in wild type (**m**) and altered spindle position and organelles spread throughout the cells in *ps1*(**n**) and *jas* (**o**) mutants; anaphase II with separating sister chromatids (**p**–**r**). Anthers were from wild type (WT; **a**, **d**, **g**, **j**, **m**, **p**), *ps1* (**b**, **e**, **h**, **k**, **n**, **q**) and *jas* (**c**, **f**, **i**, **l**, **o**, **r**) plants. Images are projections of 3 or 4 optical sections. A z-series for each of these regions is provided in Online Resources 5 to 22 respectively. As meiocytes in an anther are at slightly different stages, the noted stage for each image describes the majority of the meiocytes. Scale; 10 µm

products from the *ps1* mutant (d'Erfurth et al. 2008). Additionally, differences can be seen in the position of organelles in *jas*. The organelles with DNA are clustered in a region of the cytoplasm, close to but excluded from the spindle during meiosis I in wild-type meiocytes, but are distributed throughout the meiocyte in *jas* but not in *ps1,* as previously reported (Brownfield et al 2015).

Following meiosis I, the chromosomes decondense at interphase and the organelles are located between the two chromosomes groups (Fig. 3j–l, Online Resources 14–16). Both the *ps1* and *jas* mutants are similar to wild type at this stage, as previously reported (Brownfield et al 2015).

As simultaneous cytokinesis occurs male meiosis in *A. thaliana*, there are two chromosome divisions occurring in one cell during meiosis II (De Storme and Geelen 2013). The positioning and orientation of the two spindles is crucial for the separation of chromosomes into four separate groups and subsequently nuclei, and is disturbed in the *ps1* and *jas* mutants (d'Erfurth et al. 2008; De Storme and Geelen 2011; Brownfield et al. 2015). As this technique maintains three-dimensional structure of the cells, these phenotypes can be observed, especially using the z-series (Fig. 3m–r, Online Resources 17–22). In wild-type meiocytes, the organelle band can be observed between the two chromosome groups throughout meiosis II, with the spindles organised such that the chromosome will be separated into four groups: this is often perpendicular arrangement but not in all cases (Fig. 3m, Online Resource 17). The spindle position and organelle band are disturbed in the *ps1* and *jas* mutants, with spindles often close at one or two poles and organelles distributed throughout the cells (Fig. 3n, o and Online Resources 18 and 19). Being able to follow the progression of chromosome separation stages along with observing information on cellular structure and organelle position, provides another tool to study meiosis in *A. thaliana*. It may be particularly useful as a quick preliminary analysis to identify broad phenotypes and inform further analyses, such as microtubule localisation or other organelle localisation for phenotypes such as those observed with *ps1* and *jas.*

Whole anther analysis in *M. truncatula*

Being able to easily visualise meiotic cells will be key in translating genetic and molecular knowledge from the widely studied *A. thaliana* into other plants, and crop plants in particular. Since the results with this rapid technique in *A. thaliana* were promising, we were interested if whole anthers of other plant species can also be analysed using this method, again with a focus on the chromosome separation stages.

Initially, we chose *M. truncatula* as another test species with simultaneous cytokinesis and small floral buds like *A. thaliana*. *M. truncatula* serves as a model for the legumes,

including economically important crops such as soybean, as *M. truncalula* has a small, diploid and sequenced genome and is amenable to study with a short generation time (Bell et al. 2001). Like *A. thaliana*, *M. truncatula* has relatively small buds and anthers, although the flowers do not develop in inflorescences. Therefore, for *M. truncatula* we fixed young flower buds (approximately 1 mm long) and then prepared and viewed slides in a similar manner as for *A. thaliana* (Fig. 1). Like with *A. thaliana*, entire *M. truncatula* anthers could be viewed by CLSM, with *M. tuncatula* anthers having an apple-like shape (Fig. 4 with the z-series for these anthers in Online Resource 23 and 24). Additionally, multiple locules within an anther can be observed in a single optical section. When looking at the meiotic stages, we observed that like for *A. thaliana*, the locules within an anther can contain meiocytes of different stages. For example, stages ranging from metaphase I to telophase II were observed in the locules of a single anther (Fig. 4).

Similar to A. *thaliana*, organelle DNA was also stained with DAPI in *M. truncatula* meiocytes and appeared to be organised in a similar manner. In meiosis I, the organelles were observed to be around the spindle region and the organelles were located in a band across the equator of the meiotic from the end of the first meiotic division and throughout the second division (Fig. 4). This suggests there are similar mechanism controlling the cytoplasmic organisation in *M. truncatula*, and it is possible that loss of the organelle band could also result in altered spindle position and unreduced meiotic products. Such spindle positioning defects have been observed in legumes, but the organelle location has not been examined (Tavoletti et al. 1991; Mariani et al. 2000).

The layers of the anther could also be distinguished using CLSM with *M. truncatula* anthers (Fig. 4). The supporting tapetum cells are prominent, with nuclei that are significantly larger than in *A. thaliana* tapetal cells.

Whole anther analysis in kiwifruit

Finally, we tested this method with a more challenging sample; kiwifruit. Kiwifruit is a major tree crop in New Zealand and elsewhere and genome sequence has recently become available (Pilkington et al. 2018). Additionally, kiwifruit floral buds and anthers are significantly larger than *A. thaliana* and *M. truncatula* anthers, and each kiwifruit flower has a high number of anthers.

Using buds developed from budwood in growth chambers, kiwifruit anthers were prepared for viewing with a few adaptations from the *A. thaliana* protocol (Fig. 1). As

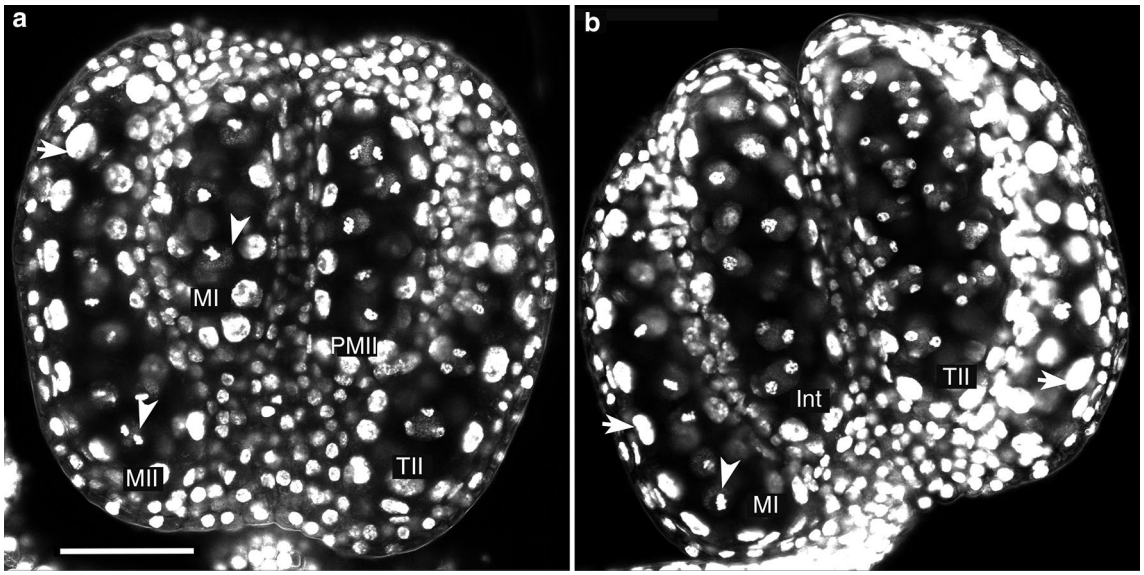

Fig. 4 CLSM analysis of meiocytes in *M. truncatula* anthers. Anthers were prepared from individual *M. truncatula* buds, chromosomal DNA and organelles stained with DAPI and observed with CLSM. **a** *M. truncatula* anther showing multiple meiosis stages in the four locules. A *z*-series for this anther is provided in Online Resource 23. From left to right locules contain: metaphase II (MII) with two groups of sister chromatids aligned and an organelle band between the chromosome groups (arrow head); metaphase I (MI) with homologous chromosomes aligned and organelles around the spindle area (arrowhead); prometaphase II (PMII) with condensed sister chromatids not yet aligned and an organelle band between the chromosome groups; telophase II (TII) with the two meiotic divisions are complete (not all four nuclei can be seen in the optical slice). **b** *M. truncatula* anther showing multiple meiosis stages in the three locules. A *z*-series for this anther is provided in Online Resource 24. From left to right locules contain: metaphase I (MI) with homologous chromosomes aligned and organelles around the spindle area (Arrowhead); Interphase (Int) between the two meiotic divisions at the bottom of the anther (Int); telophase II (TII) with the two meiotic divisions are complete. Arrows indicate tapetal cells with large nuclei. Images are single optical sections. Scale; 50 µm

kiwifruit buds are larger, more robust and have a waxy surface, we anticipated difficulties with rapid penetration of the fixative into the anthers in whole buds. We therefore took advantage of the larger anther size in kiwifruit and removed anthers likely to contain meiotic stages from buds (based on size: see Methods) and fixed the isolated anthers. The greater anther size also enabled kiwifruit anthers to be stained before being transferred to the microscope slide. We trialled clearing kiwifruit anthers using ClearSee (Kurihara et al. 2015), but this led to discoloration likely due to interactions with polyphenols, and poorer imaging with CLSM.

While anthers can be isolated by removing a bud from the cane and opening it, we found we could also cut a window through the tepals and sepals on the side of the bud and remove up to five anthers. While anthers remaining in the bud that are close to the window become dehydrated, anthers within the remainder of the bud with the window continue to develop until anthesis. This means that anthers at a later stage of development could also be removed from the same bud for analysis over time, which is useful if there is limited number of male buds available.

The greater anther size in kiwifruit meant that only two locules of each anther was able to be viewed with our CLSM setup under low magnification (not shown), and only one locule imaged at a time under higher magnification (Fig. 5). Each kiwifruit locule contained more meiocytes than a locule from *A. thaliana* or *M. truncatula* (compare Figs. 2, 4 and 5). The two locules observed from a kiwifruit anther generally contained the same stage, with most of the anthers observed containing tetrads (Fig. 5a), suggesting this is a long duration in kiwifruit.

We observed some locules in which meiocytes were undergoing the chromosome separation stages (Fig. 5b). With the high number of meiocytes in a locule, it was noticeable that meiocytes in an anther are at different stages of meiosis. In a single locule, cells at either end were in the early stages of meiosis I (metaphase on the left and prometaphase on the right of Fig. 5b) with later stages (late anaphase I) near the centre (Fig. 5b). Thus, it appears that cells in the centre of a locule are slightly further ahead in meiotic progression that the cells closer to the ends. Our observations (not shown) suggest that this may not relate to the longitudinal distribution, but distance from the tapetum as in different optical sections those cells closer to the tapetum in the middle of the locule also appeared to be at an earlier developmental stage. This suggests that there could be some form of signalling between meiocytes and the tapetum in each locule.

Like with *A. thaliana* and *M. truncatula*, the layers of the anther can also be observed in the CLSM of kiwifruit anthers (Fig. 5). Kiwifruit anthers, however, differ from *A. thaliana* and *M. truncatula* in that the middle layer consists of two cell layers rather than a single layer (Falasca et al. 2013).

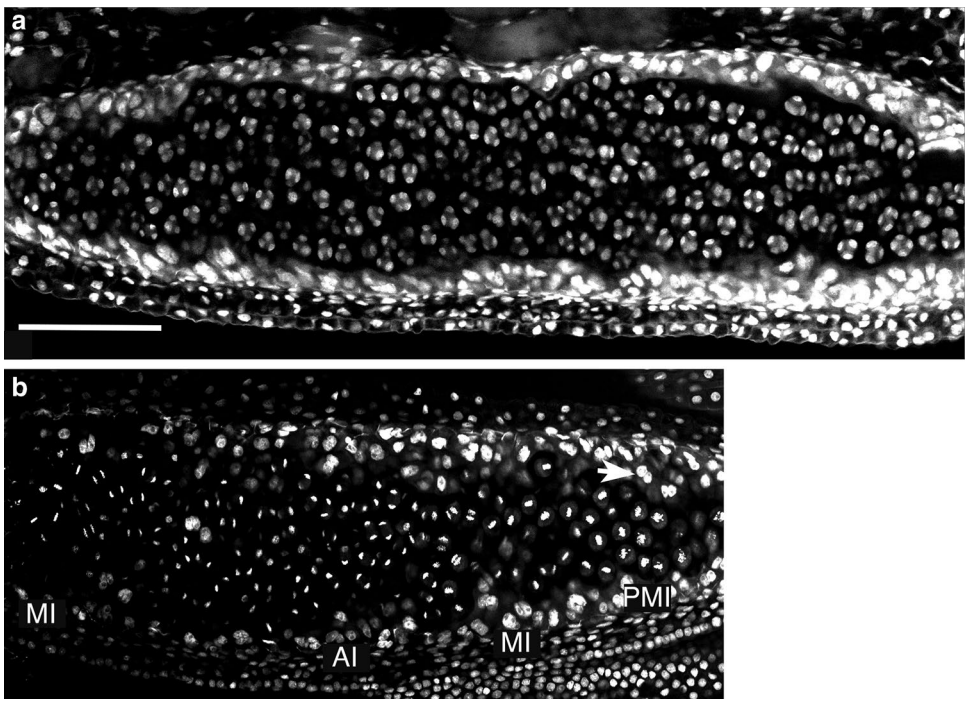

Fig. 5 CLSM analysis of meiocytes in kiwifruit anthers. Anthers were removed from kiwifruit flower buds, chromosomal DNA and organelles stained with DAPI and observed with CLSM. **a** A locule with tetrads. The tapetum has begun to degrade by this stage. **b** A locule with meiocytes in meiosis I. Towards the ends of the locule the meiocytes are in the early stages of meiosis I (prometaphase I (PMI) and metaphase I (MI)), while in the middle at the later stage of anaphase I (AI). A binucleate tapetal cells is indicated by an arrow. Images are single optical sections. Scale; 100 µm

Conclusion

The protocol described here is a short and simple way of analysing male meiotic cells within anthers. It provides a technique to easily fix material, prepare slides and view with a standard CLSM set up. By retaining the meiocytes in the anthers, many meiotic cells can be imaged simultaneously allowing comparison of many cells in different genotypes, the three-dimensional structure and cytoplasmic information (such as the position of organelles) is maintained, and the synchrony of meiosis can be observed. The adaptability and rapidness of this protocol will make it particularly useful as a preliminary screen of mutants or treatments to help researchers identify the aspect of meiosis impacted and inform further analyses. Additionally, the technique could be further modified to view different aspects of meiotic cells. This could be relatively small modifications such as altering the imaging set up to provide optimal exposure of the target cell type or chromosomal structure or more substantial modifications such as by the use of stains other than DAPI, like analine blue or calcofluor, to look at cell wall material or fluorescence in situ hybridization.

The technique was developed in the model plant *A. thaliana* which has small buds and anthers, and we have shown is can be used in other plants with both small floral organs (using *M. truncatula*) and larger more robust floral organs (using kiwifruit). Thus, by considering the floral structure and the size of anthers and deciding whether to fix and stain whole buds or anthers, researchers working in a range of plants, including non-model crops plants, could adopt this simple technique to view male meiotic cells.

Supplementary Information The online version contains supplementary material available at (https://doi.org/10.1007/s00497-021-00404-5).

Acknowledgements We would like to thank Shona Seymour at Plant & Food Research for the collection of kiwifruit budwood. This work was funded by the Department of Biochemistry, University of Otago, New Zealand and the Endeavour Fund from the Ministry of Business Innovation and Employment (Smart Idea UOOX1801).

Author's contribution statement CR carried out research, analysed data, wrote the manuscript. LLL carried out research, analysed data, SP designed and supported research. LB designed and carried out research, analysed data, wrote the manuscript. All authors read and approved the manuscript.

Funding Department of Biochemistry, University of Otago and Ministry of Business Innovation and Employment Endeavour Fund (Smart Idea UOOX1801).

Availability of data and materials Additional electronic material is available online.

Compliance with ethical standards

Conflict of interest The authors declare that they have no conflict of interest.

References

Armstrong SJ, Franklin FCH, Jones GH (2003) A meiotic time-course for *Arabidopsis thaliana*. Sex Plant Reprod 16:141–149. https://doi.org/10.1007/s00497-003-0186-4

Barker DG, Pfaff T, Moreau D, Groves E, Ruffel S, Lepetit M, Whitehand S, Maillet F, Nair RM, Journet EP (2006) Growing *M. truncatula*: choice of substrates and growth conditions. In: *Medicago truncatula* Handbook, version November 2006, Noble Research Institute. ISBN 0-9754303-1-9

Bell CJ, Dixon RA, Farmer AD, Flores R, Inman J, Gonzales RA, Harrison MJ, Paiva NL, Scott AD, Weller JW, May GD (2001) The Medicago genome initiative: a model legume database. Nucleic Acid Res 29:114–117. https://doi.org/10.1093/nar/29.1.114

Bennett MD, Chapman V, Riley R (1971) The duration of meiosis in pollen mother cells of wheat, rye and *Triticale*. Proc R Soc Lond Ser B 178:259–275. https://doi.org/10.1098/rspb.1971.0065

Brownfield L, Jun Y, Jiang H, Minina EA, Twell D, Köhler C (2015) Organelles maintain spindle position in plant meiosis. Nat Comms 6:6492. https://doi.org/10.1038/ncomms7492

Cabout S, Leask MP, Varghese S, Yi J, Peters B, Conze LL, Köhler C, Brownfield L (2017) The meiotic regulator JASON utilizes alternative translation initiation sites to produce differentially localized forms. J Exp Bot 68(5):4205–4217. https://doi.org/10.1093/jxb/erx222

Caporali E, Testolin R, Pierce S, Spada A (2019) Sex change in kiwifruit (*Actinidia chinensis* Planch.): a developmental framework for the bisexual to unisexual floral transition. Plant Reprod 32:323–330. https://doi.org/10.1007/s00497-019-00373-w

Cardarelli M, Cecchetti V (2014) Auxin polar transport in stamen formation and development: how many actors? Front Plant Sci 5:333. https://doi.org/10.3389/fpls.2014.00333/full

Chelysheva L, Diallo S, Vezon D, Gendrot G, Vrielynck N, Belcram K, Rocques N, Marquez-Lema A, Bhatt AM, Horlow C, Mercier R, Mezard C, Grelon M (2005) AtREC8 and AtSCC3 are essential to the monopolar orientation of the kinetochores during meiosis. J Cell Sci 118:4621–4632. https://doi.org/10.1242/jcs.02583

Colas I, Darrier B, Arrieta M, Mittmann SU, Ramsay L, Sourdille P, Waugh R (2017) Observation of extensive chromosome axis remodelling during the "diffuse-phase" of meiosis in large genome cereals. Front Plant Sci 8:1235. https://doi.org/10.3389/fpls.2017.01235

Crismani W, Girard C, Mercier R (2013) Tinkering with meiosis. J Exp Bot 64:55–65. https://doi.org/10.1093/jxb/ers314

d'Erfurth L, Jolivet S, Froger N, Catrice O, Novatchkova M, Simon M, Jenczewski E, Mercier R (2008) Mutations in *AtPS1* (*Arabidopsis thaliana Parallel Spindle 1*) lead to the production of diploid pollen grains. PLoS Genet 4:e1000274. https://doi.org/10.1371/journal.pgen.1000274

De Storme N, Geelen D (2011) The Arabidopsis mutant *jason* produces unreduced first division restitution male gametes through a parallel/fused spindle mechanism in meiosis II. Plant Physiol 155:1403–1415. https://doi.org/10.1104/pp.110.170415

De Storme N, Geelen D (2013) Cytokinesis in plant male meiosis. Plant Signal Behav 8:e23394. https://doi.org/10.4161/psb.23394

Erilova A, Brownfield L, Exner V, Rosa M, Twell D, Mittelsten Scheid O, Hennig L, Köhler C (2009) Imprinting of the polycomb group

gene medea serves as a ploidy sensor in arabidopsis. PLoS Genet 5(9):e1000663. https://doi.org/10.1371/journal.pgen.1000663
Falasca G, D'Anheli S, Biasa R, Fattorini L, Matteucci M, Canini A, Altamura MM (2013) Tapetum and middle layer control male fertility in *Actinidia deliciosa*. Ann Bot 112:1045–1055
Fransz P, Armstrong S, Alonso-Blanco C, Fischer TC, Torres-Ruiz RA, Jones G (1998) Cytogenetics for the model system *Arabidopsis thaliana*. Plant J 13(6):867–876. https://doi.org/10.1046/j.1365-313X.1998.00086.x
Goldberg RB, Beals TP, Sanders PM (1993) Anther development: Basic principles and practical applications. Plant Cell 5:1217–1229
Harrison CJ, Alvey E, Henderson IR (2010) Meiosis in flowering plants and other green organisms. J Exp Bot 61:2863–2875. https://doi.org/10.1093/jxb/erq191
Kurihara D, Mizuta Y, Sato Y, Higashiyama T (2015) ClearSee: a rapid clearing reagent for whole-plant fluorescence imaging. Development 142:4168–4179
Lambing C, Heckmann S (2018) Tackling plant meiosis: from model research to crop improvement. Front Plant Sci. https://doi.org/10.3389/fpls.2018.00829
Lei X, Liu B (2020) Tapetum-dependent male meiosis progression in plants: increasing evidence emerges. Front Plant Sci. https://doi.org/10.3389/fpls.2019.01667
Li J, Dukowic-Schulze S, Lindquist IE, Farmer AD, Kelly B, Li T, Smith AG, Retzel EF, Mudge J, Chen C (2015) The plant-specific protein FEHLSTART controls male meiotic entry, initializing meiotic synchronization in Arabidopsis. Plant J 84:659–671. https://doi.org/10.1111/tpj.13026
Mariani A, Campanoni P, Giani S, Breviario D (2000) Meiotic mutants of *Medicago sativa* show altered levels of α- and β-tubulin. Genome 43:166–171. https://doi.org/10.1139/g99-105
Nair RM, Peck DM, Dundas IS, Samac DA, Moore A, Randles JW (2008) Morphological characterisation and genetic analysis of a bi-pistil mutant (*bip*) in *Medicago truncatula* Gaertn. Sex Plant Reprod 21:133–141. https://doi.org/10.1007/s00497-008-0073-0
Pilkington SM, Crowhurst R, Hilario E, Nardozza S, Fraser L, Peng Y, Gunaseelan K, Simpson R, Tahir J, Deroles SC et al (2018) A manually annotated *Actinidia chinensis* var. *chinensis* (kiwifruit) genome highlights the challenges associated with draft genomes and gene prediction in plants. BMC Genom 19:257. https://doi.org/10.1186/s12864-018-4656-3
Prusicki MA, Keizer EM, van Rosmalen R, Komaki S, Seifert F, Mueller K, Wijnker E, Fleck C, Schnittger A (2019) Live cell imaging of meiosis in *Arabidopsis thaliana*. eLIFE 8:e42834. https://doi.org/10.7554/eLife.42834
Sanders PM, Bui AQ, Weterings K, McIntire KN, Hsu Y-C, Lee PY, Truong MT, Beals TP, Goldberg RB (1999) Anther developmental defects in Arabidopsis thaliana male-sterile mutants. Sex Plant Reprod 11:297–322. https://doi.org/10.1007/s004970050158
Scott RJ, Spielman M, Dickinson HG (2004) Stamen structure and function. Plant Cell 16:S46. https://doi.org/10.1105/tpc.017012
Smyth DR, Bowman JL, Meyerowitz EM (1990) Early flower development in Arabidopsis. Plant Cell 2:755–767. https://doi.org/10.1105/tpc.2.8.755
Tavoletti S, Mariani A, Veronesi F (1991) Cytological analysis of macro- and microsporogenesis of a diploid alfalfa clone producing male and female 2n gametes. Crop Sci 31:1258–1263. https://doi.org/10.2135/cropsci1991.0011183X003100050035x
Wilson ZA, Song J, Taylor B, Yang C (2011) The final split: the regulation of anther dehiscence. J Exp Bot 62:1633–1649